ФІЗИКА І ХІМІЯ ТВЕРДОГО ТІЛА
Т. 18, № 2 (2017) С. 166-172
DOI: 10.15330/pcss.18.2.166-172

PHYSICS AND CHEMISTRY OF SOLIDSTATE
V. 18, № 2 (2017) P. 166-172

PACS: 78.67.Bf, 78.55.-M, 87.85.RS, 87.85.FK, 87.14.E

ISSN 1729-4428

I.D. Stolyarchuk[1], R. Wojnarowska - Nowak[2], J. Polit[2], E. Sheregii[2], S. Nowak[3], M. Romerowicz - Misielak[3]

CdTe Quantum Dots and Their Bioconjugate with Human Serum Albumin for Fluorescence Imaging

[1]Department of Theoretical and Applied Physics and Computer Simulations,Ivan FrankoDrohobych State Pedagogical University, 24 I. Franko str., 82100 Drohobych, Ukraine, e-mail: istolyarchuk@ukr.net
[2]Centreof Microelectronics and Nanotechnology, University of Rzeszow, 1 Pigonia Street, 35959 Rzeszow, Poland, e-mail: wojnarowska.renata@gmail.com, polijack@ur.edu.pl
[3]Department of Physiology and Reproduction of Animals, Institute of Applied Biotechnology and Basic Sciences, University of Rzeszow, Werynia 502, Kolbuszowa, 36-100, Poland, e-mail: slawomir.urz@gmail.com, romerowicz@ur.edu.pl

The interaction between CdTe quantum dots (QDs) with human serum albumin (HSA) and human cell culture was studied by optical spectroscopy technique. Performed research explored the interaction between the CdTe QDs and HSA, and fluorescence imaging efficiency of the QD-HSA bioconjugates in comparison with colloidal QDs. The secondary structure of the HSA is similar to the native form, which suggest a biocompatibility of prepared bionanocomplex. The CdTe QD-HSA bionanoconjugate shows chemical stability in phosphate-buffered saline (PBS) under ambient conditions, furthermore, it is stable in cytoplasm and suitable for cell labeling, tracking, and other bioimaging applications. The CdTe QDs located in an osteosarcoma cancer cells show a high luminescence intensity. The light emission of the CdTe QDs connected with albumin is less than the pure QDs, but it is still satisfactory, and additionally it is stable and have long photoluminescence lifetime. It suggest, that the CdTe NC-HSA bionanocomplex can be used as a fluorescent probe for cell labeling, tracking, and other bioimaging applications.

Keywords: CdTe, quantum dot, nanoparticles, human serum albumin, fluorescence quenching,osteosarcoma cancer cell, bionanocomplex, bioconjugate, bioimaging.

Стаття поступила до редакції07.11.2016; прийнята до друку 05.06.2017.

Introduction

Nanotechnology plays a central role in the recent technological advances in the areas of disease diagnosis, drug design and drug delivery. The nanotechnological applications to disease treatment, diagnosis, monitoring, and to the control of biological systems have been referred to as "*nanomedicine*"[1,2]. Nanomedicine needbiologically relevant nanostructures including semiconductor nanoparticles, magnetic nanoparticles, carbon-based nanostructures and metallic nanoparticles. Research on semiconductor nanocrystals (NCs), also known as quantum dots (QDs), and their application in nanomedicine, has intensified rapidly in the past few decades [3-10].

QDs are useful as a novel probe in biosensors as well as for bio-imaging due to unique size dependent their optical and electrical properties. Moreover, semiconductor QDs are also becoming valuable analytical tools for nanomedicine as they offer the opportunity to design luminescent probes for labeling, imaging, and sensing with unprecedented performance [4].From a point of view of biomedical applications the II-VI based QDs have particular interest due to broad absorption spectra, narrow photoluminescence spectra, size-tunable spectra and high sensitivity. These nanoparticles are brightly fluorescent, enabling their use as imaging probes both *in vitro* and *in vivo*study [5].Moreover, a semiconductor QDs are able to fluorescence resonance energy transfer process (FRET) and by this effect can be commonly used as a biological molecular probes [3]. In composition with other chemicals or materials their optical properties could be easily modified [6, 7].

There has been increasing interest in estimating the toxicity of the II-VI based undoped (as well as doped) QDs because the tremendous focus on these nanoparticles due to their biological and biomedical

applications. However, the toxicity of QDs including CdTe QDs can be minimized by their composition with a biocompatible shell [8].

It is well known that the human serum albumin (HSA) is the most abundant protein in blood plasma which is involved in the transport of a variety of endogenous and exogenous ligands [9]. Transportation, distribution, physiological and toxicological actions of the ligands *in vivo*are closely related to their binding with proteins. Several reports have been devoted to study such kind of interaction between the II-VI based nanoparticles and HSA as well as bovin serum albumin (BSA) [9-14]. So, it is very significant for nanomedicine to investigate the interaction between the nanoparticles and the major carrier protein like BSA and HSA.

One of nanomedicine applications of the II-VI based QDs is earlier diagnostic of cancer cells including osteosarcoma cells. Osteosarcoma is the primary malignant tumor of bone in adult, young people and children.Patient's5-year survival rate is between 50 to 63 % [15]. The tumor is frequently localized in femur and tibia bones, but the cancer diagnosis is very difficult and often too ineffective. Researchers proved that osteosarcoma cells have numerous genetics' mutations and other abnormalities, which additionally hinders the effective diagnosis and treatment [16]. Early detection is particularly important, because the tumor is prone to metastasize (especially in the lung). The human osteosarcoma cell line was selected to determine the interaction of the CdTe QDs with human cancer cells [17].To improve the cancer detection and treatment effectiveness, researches on the cell lines with nanoparticles are conducted increasingly [9-18].

In our previous short communication [19,20] the results onoptical spectroscopy in the region of the fundamental absorption edge of the CdTe QDs connected with HSA as well as the photoluminescent spectra of some size of QDs, were presented. In the present work, the results of research dedicated to the CdTe quantum dots interaction with human serum albumin and human cell culture are reported. Particularly, the size and temperature influence on these interactions is considered in wide region of these parameters. The different methods are used for this aim: the UV-VIS absorption and fluorescence spectroscopy(as well as fluorescence microscopy)as main methods, complemented by Infrared and Raman spectroscopy for chemical functional groups identification, and detection of changes in protein secondary structure through changes in oscillation spectra. Prepared constructs of different concentrations of CdTe QDs under interaction with HSA protein as well as pure CdTe QDs are investigated to found an optimal product for human cancer cells bio-imaging.

I. Experimental

Nanoparticles of CdTe were prepared in aqueous solution at room temperature using procedure similar to described in [17,18]. Briefly, Cd precursor solutions were prepared by mixing 3 mmol of $CdCl_2$ with 225 ml of ultrapure water followed by 7.7 mmol of thioglycolic acid (TGA) under magnetic stirring. The pH value of the mixed solution was adjusted to 10.0 by dropwise addition of 1MNaOH solution. Then, gas mixture of Ar and H_2Te was passed through the solution. The reaction time was varied to achieve different molar ratio of Cd^{2+}:Te^{2-}:TGA.

Transmission electron microscopy (TEM) was used in order to confirm the structure of the grown nanoparticles: estimate shape and determine the average size of nanocrystals as well as their composition and crystal structure. A TEM instrument Tecnai Osiris X-FEG TEM microscopy that provides maximum resolution of 0.136 nm has been used. For this kind of microscopic analysis a drop of colloidal suspension was placed on special carbon-coated copper grid.

HSA was purchased from PJSC Biofarma (Ukraine) at the concentration of $1.5x10^{-6}$ mol l^{-1}. Solutions of CdTenanocrystals with HSA were prepared by adding the set amount of quantum dots (from 0.1 x 10^{-6} $moll^{-1}$to 1.9 10^{-6} mol l^{-1}) to fixed volume of HSA (1 ml) and stirred for 2 min. The experiments were started in 10 min after the sample preparation. It allow to achieve the temperature equilibration.

The absorption spectra of HSA, CdTe QDs and HSA–QDs solutions were recorded at room temperature, with using a UV-VIS Evolution 300 (Thermo Scientific) spectrophotometer. Whereas, photoluminescence spectra of the colloidal CdTe QDs, pure HSA solution and HSA under interaction with different concentrations of the QDs (0.6; 0.9; 1.5 10^{-6}mol l^{-1} of QDs), were measured by means of F-2500 Hitachi spectrofluorymeter, equipped with a 1.0 cm quartz cell. An excitation radiation with wavelength of 325 nm was chosen to record the emission intensity in the wavelength region from 350 to 850 nm at room temperature.

The oscillation spectra are obtained using Fourier transform infrared (FTIR) spectrometer Vertex 70v (Bruker) applying the Attenuated Total Reflectance (ATR) technique. The measurements were performed with 60 scans, and the 1 cm^{-1}spectral resolution. The Raman spectra were acquired with the Smart Raman DXR (Thermo Scientific) spectrometer in narrow spectral range of 1000 – 1800 cm^{-1}. The 14 mWpower and 780 nm wavelength semiconductor laser was used as a light source.

The human bone osteosarcoma 143b cells were maintained in Dulbecco's Modified Eagle's medium (DMEM), supplemented with: fetal bovine serum (FBS) (10%), and penicillin-streptomycin (1%) antibiotic. The cells were incubated in 5% CO_2 at 37^{o}C. The cells were collected and centrifuged for 7 min, at 4°C, at 600 g force. Then, the cells were seeded in a 96-well plate at a density of 8.0×10^4 cells per ml, and incubated during 24h. The CdTe QDs were mixed with DMEM medium to 8, 20, $30x10^{-5}$mol $l^{-1}$of QDs concentration. An aliquot (100µl) of prepared solution was added to each well, and incubated by 3, 6, 9 and 24h.In the next experiment of the QDs-cell interaction, osteosarcoma cells were fixed by pre-cooled methanol and the cell membrane was permeated by incubating in 0.1% Triton X-100 reagent. In this case of experiment CdTe nanoparticles were mixed with phosphate-buffered saline (PBS buffer), and 100µl aliquot was added to cell culture, and incubated for 10 minutes.

The fluorescence ability of the CdTeQDs under

interaction with additional amount of albumin (inside cancer cells) were also investigated. Cell nuclei were stained with Hoechst 33342 fluorescent dye, for 5 min, at room temperature, in the dark. The image were taken by In Cell Analyzer 2000 automated microscope (GE Healthcare, UK). Image were taken with two different excitation/emission filters (543/605 nm for CdTe QDs and 350/455 nm for Hoechst 33342 dye).

II. Results and Discussion

The TEM and HR TEM images of typical colloidal CdTe nanoparticles are shown in Fig. 1.In insert of Fig. 1 is shown an atom-resolved image of one CdTe-QD. As can be seen the shape of the nanoparticles is close to spherical and the average diameter of the nanoparticles is found to be approximately from 2.5 to 3.2 nm. It is seen in insert the crystalline structure of QDs is perfect. Averaged size of bionanoconjugates (or bionanocomplexes) were confirmed by AFM measurement, and it was about 10-15 nm.

For the evaluation of optical properties of pure QDs, pure HSA and QDs CdTe-HSA complex absorption spectra are recorded and analyzed. An addition of HSA to colloidal CdTe nanoparticles leads to a gradual decrease of optical density and broadening of exciton structure [20]. However, energy position of the exciton bands is not shifted. The obtained results indicate that the binding process between the QDs and the protein molecules change not the electron states in the QD.

Photoluminescence spectra of HSA under interaction with QDs have been recorded on spectrofluorymeter upon excitation wavelength optimal for the investigated QDs which is dependent on their size and shape resulting in a certain position of absorption bands. The photoluminescence intensity of HSA progressively decreases with increasing of the of CdTe QDs

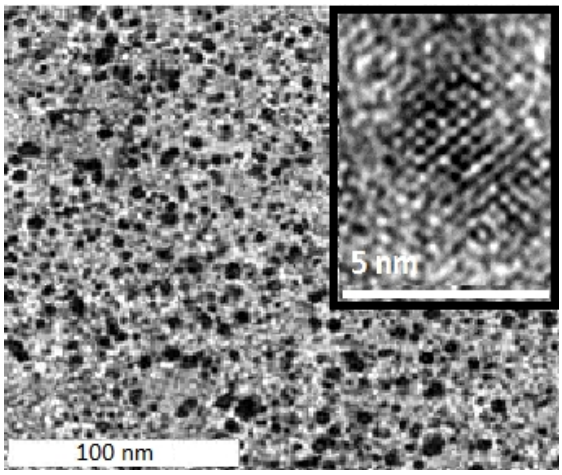

Fig. 1. TEM and HR TEM (insert) images of the colloidal CdTe quantum dots.

concentration. Fluorescence quenching is a powerful tool to characterize changes of the optical properties and determine the type of interaction between protein and quenchers in solution. The photoluminescence quenching mechanism for quantum dots can be determine from the Stern-Volmer equation. Obtained results, as in [19, 20] suggest that the nature of quenching is static, resulting in forming QDs CdTe-HSA bionconjugates.

Infrared and Raman spectroscopy are complementary techniques and they are commonly used for the chemical structure determination of molecules as well as the conformation changes and interaction between molecules [21, 22]. For analyze the oscillation spectra of the HSA, and tested the changes of the HSA structure after interaction with CdTe QDs, at first the FTIR spectroscopy was investigated. The obtained results are shown in Fig. 2 and presented in Table 1.

Infrared spectra of HSA contains typical lines corresponding to amide bands of proteins. Amide I band

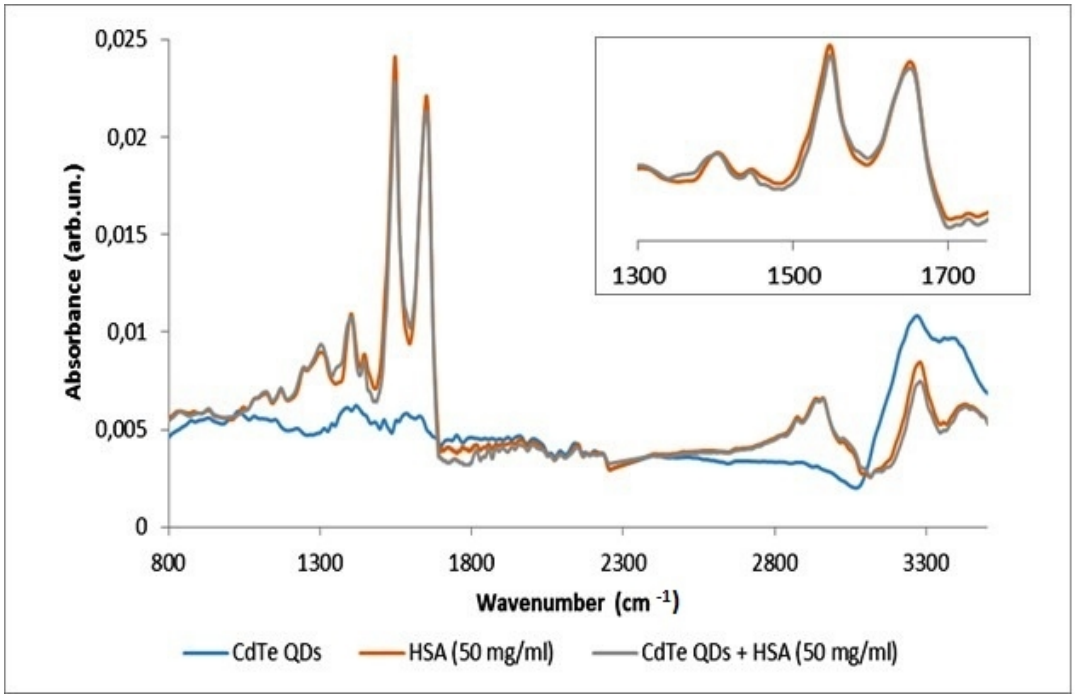

Fig. 2. FTIR spectra of the CdTe QDs (blue), HSA (red), HSA after interaction with CdTe QDs (grey).

Table 1

Identification of the lines observed in the FTIR spectra of HSA (Fig. 5); s-strong, m-medium, w-weak

	Position of line (cm^{-1})	Identification	Reference
1	3429 (m)	O-H stretch	24, 25
2	3278 (m)	N-H stretch	24-26
3	2960, 2934, 2873 (m)	C-H stretch (asymmetric and symmetric methyl-)	24, 25
6	1650 (s)	Amide I (**C=O** stretch, CN stretch, CCN deformation, NH bend)	23, 24, 26
7	1547 (s)	Amide II (**NH** bend, **CN** stretch, CO in plane, CC, NC stretch)	23, 24, 26
8	1446(w)	C-H bend	24, 25
9	1402 (m)	COO- stretch and C-H bend	24, 26
10	1319 (m)	O-H bend	25
11	1259 (w)	Amide III (**CN** stretch, **NH** bend, CO in plane, CC stretch)	23, 24, 26
13	1129 (w)	skeleton vibration	25, 26

mainly occurs in the region of 1600 to 1700 cm^{-1} and amide II band in the region of 1500-1550 cm^{-1}. Amide I corresponds mainly to the stretching vibration of peptide carbonyl group (C=O), but also to CN stretching, CCN deformation, NH bending vibrations. Amide II band is attributed to C–N stretching coupled with N–H bending vibrations and in less intense to CO, CC, NC stretching vibrations [23, 24]. Apart from these two main lines, other characteristic signals for the HSA protein were reported. The weak line observed at 1259 cm^{-1}corresponds to the amide III band and it can be assigned mainly to CN stretching, and NH bending a vibrations [23, 24].The region from 2800 cm^{-1} to 3600 cm^{-1} is also interesting, and associated with the bands corresponding to C-H , N-H and O-H stretching vibrations [25]. The N-H vibration lines recorded at 3278 $cm^{-1}$and 3070 cm^{-1} (very weak) are named amide A and amide B [26]. The line attributed to O-H bonds is observed approximately at 3429 cm^{-1}, and C-H bands at around 2960cm^{-1}, 2934cm^{-1}, 2873 cm^{-1}, (stretching vibration) as well as at 1446 cm^{-1}(bending vibration) [24, 25]. Other bands are assigned to the chemical group of the amino acids in the HSA protein and to molecule's skeleton. The most unique for each sample is the region from 500 to 1300 cm^{-1}, it is called as the fingerprint region [23, 25].

Both of the amide I and amide II lines indicate the secondary structure of protein (especially amide I)[27, 28]. Shifting of position of the peak maximum is not large, from 1650 $cm^{-1}$to 1652 $cm^{-1}$for amide I and from 1547 $cm^{-1}$to 1548 $cm^{-1}$for amide II. However, the peak's shapes and peak's intensity slightly changed also, and confirmed only slightly modification in the secondary structure of the HSA protein after interaction with the CdTe QDs. In the region from 1200 to1500 cm^{-1}, described as amide III region the structural changes were noticed also [29].Collected Raman spectra confirmed results based on the analysis of infrared spectra. The major line observed at 1657 cm^{-1}in Raman spectra and at 1650 cm^{-1} for FTIR spectra assigned to the amide I bonds is characteristic for the α-helical protein structure [23]. α-helix and β sheets are the most common type of secondary structure of protein. The α-helix is coiled in a right-handed structure, and is stabilized by hydrogen bonding occurs between successive turns of the helix. In β sheets conformation (named zig-zag) an amino acids lie either parallel or antiparallel to one another, and the hydrogen bonds are localized between the strands [30].The mentioned amide I line was shifted from 1650 to 1652 cm^{-1} in FTIR spectra and from 1657 cm^{-1} to 1651 cm^{-1}in Raman spectra, and its intensity decreased, indicating a slight reduction of α-helical folding protein type. That means HSA conformation is not much changed, and the protein structure is similar to natural one.

In order to prove that the CdTe QDs and CdTe QDs connected with HSA are useful for bio-imaging, their performance as fluorescent labels have been investigated. The pure CdTe nanoparticles without surface modification do not penetrate into the living cells. However, some of the cells in the culture has a relatively higher uptake of the QDs, and they fluorescence inside cell was noticed. Probably, they were dead and damaged cells. This suggest, that pure CdTe QDs can be used like a marker for determination of vitality of the damaged cell.

The surface of quantum dots can be modified, for improving fluorescence properties as well as the endocytosis process [31, 32]. In [32] the thiol-capped CdTe QDs proved to be a good fluorescence marker for study of cell cycle of some human carcinoma cell lines. In first step of presented study the CdTe QDs were not modified, but the cells are fixed or permeabilized by standard laboratory methods, for increasing cell membrane permeability. Methanol-fixed 143b osteosarcoma cells treated with QDs give stained interior of the cells, including nuclear region (Fig.3). The fluorescence of the CdTe quantum dots is strong and clearly visible as orange color in Fig. 3 (a) and Fig. 3 (b), even in the lowest concentrations of CdTe QDs ($8x10^{-2}$ mmol l^{-1}). The Hoechst 33342 fluorescent dye was used like a standard for cell nucleus localization, it is visible as blue color in Fig. 3(a) (weaker than quantum dots), and Fig. 3(c).

Permeabilization of cell membrane by Triton X-100 increased cell labeling, and uptake of CdTe QDs. It was demonstrated by strong quantum dots fluorescence, especially within the nucleusregion, near the center of cell (Fig.4 c,d). After cells treatment by the CdTe QDs connected with albumin, less fluorescence intensity than CdTe without the protein was observed. However, the

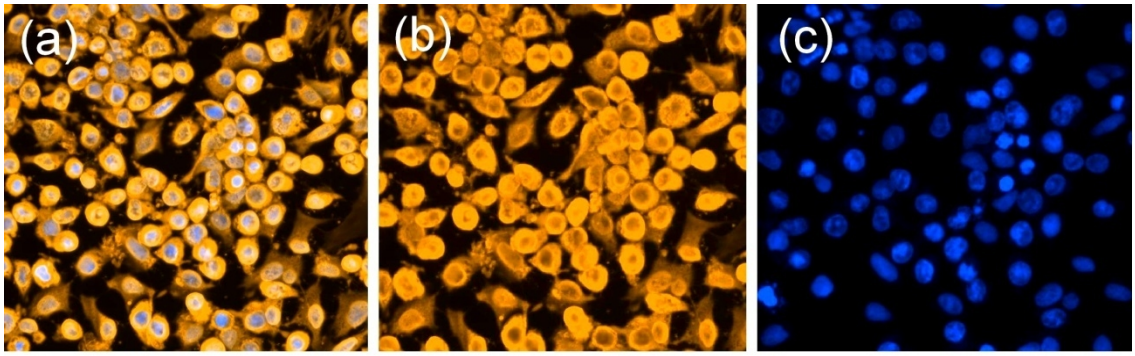

Fig. 3. Osteosarcoma cells incubated with CdTe QDs and Hoechst 33342 fluorescent dye: orange color - CdTe QDs (a and b),blue color - Hoechst 33342 fluorescent dye (a and c).

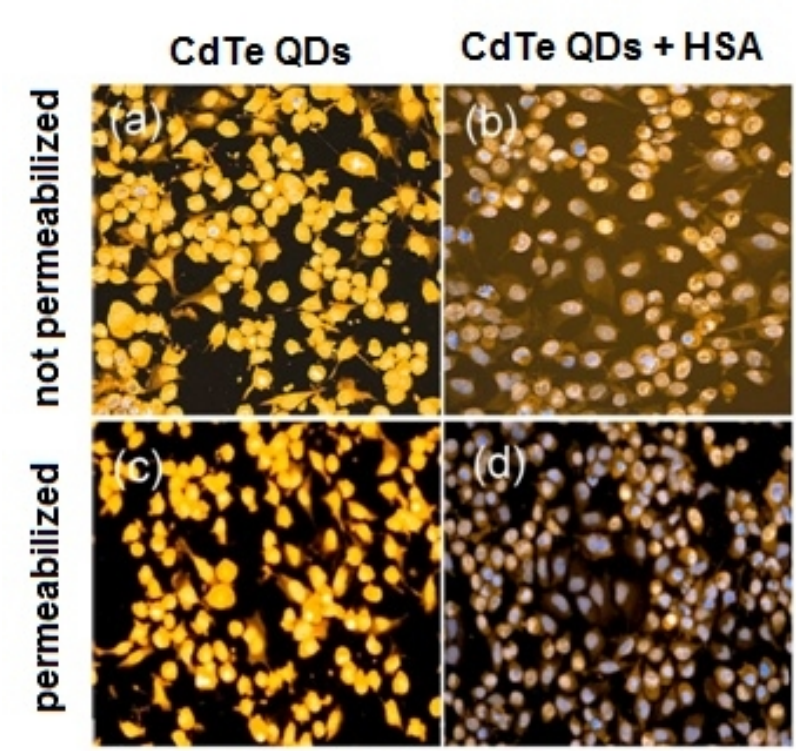

Fig. 4. Osteosarcoma cells treated by (a) CdTe QDs without HSA, without cell permabilization; (b) CdTe QDs with HSA, without cell permabilization; (c) CdTe QDs without HSA, with cell permabilization; (d) CdTe with HSA, with cell permabilization.

fluorescence efficiency was still satisfactory and it provides opportunities for bio-imaging applications of this material (Fig. 4; $8x10^{-2}$mmol $l^{-1}$of CdTe QDs concentration).

CdTe QDs show chemical stability in PBS buffer under ambient conditions. Furthermore, the intracellular CdTe QDs can be imaged by strong fluorescence even after several days. As was demonstrated by Zheng et al. [33] glutathione-coppedCdTe QDs were stable in cytoplasm and suitable for cell labeling, tracking, and other bioimaging applications. The conduct study also confirmed utility of pure QDs and QDs connected with human serum album for bioimaging of human carcinoma cells. Under the same procedure, there was no detectable emission from the control cells (without QDs in medium). Additionally, morphology of the cells treated with defined concentrations of CdTe QDs under standard conditions was not changed, compared to the control. This indicates the very low toxicity of the CdTe QDs in the case of presented bio-imaging marker. Toxic effect can comes from the disintegration of nanoparticles on toxic cadmium ions, therefore short time of exposition or nanoparticles covering partially prevents the toxic effect [8,34].

Obtained results confirmed a good luminescence intensity, stability and long photoluminescence lifetime of CdTe QDs as well as CdTe QD-HSA. BSA and HSA are often used to modify the surface of nanoparticles, including semiconductors nanoparticles [22], and leads to increase of its biocompatibility. The photoluminescence properties of prepared construct were still strong and they are useful for bioimaging of osteosarcoma cells. The CdTe QDs were mainly localized in nuclear region, what can be useful for labeling this part of cell. The QDs could be used for marking and tracking other organelles or

molecules, with additional biofunctionalization.

Conclusions

In summary, CdTe QDs with average radiuses of 3 nm were obtained by chemical colloidal method, conjugated with human serum albumin to create CdTe QDs-HSA bionanocomplex. The potential ability to cancer cells bioimaging was examined. Quenching effect of QDs fluorescence is noticed, but the fluorescence properties are still satisfactory. Obtained data enable us to find optimal concentration of the CdTe QDs-HSA bioconjugate: 20×10^{-5} M. However, it is strongly associated with the concentration of HSA. The covering of QDs by protein reduce the ability of photoluminescence, but it is still at a high level. Through the use of a natural human protein with native structure, the marker is more biocompatible, and would have less cytotoxicity. The low toxicity as well as high stability and long fluorescence lifetime of the CdTe QDs-HSA bionanocomplex in the case of their using as bioimaging probes for the 143b osteosarcoma cells is demonstrated. The results suggest that CdTe QDs-HSA bioconjugate can be potentially employed for bioimaging osteosarcoma cells with minimal adverse effect.

Stolyarchuk I.D. **–** Dr.Phys.-Math.Sci., Ass. Prof. of the theoretical and Applied Physics and Computer Modelling;
Vojnarovska-Novak R. **–** PhD-student;
PolitY. – Prof., Dr.Phys.-Math.Sci.;
Sheregiy E. – Prof., Dr.Phys.-Math.Sci.;
Novak S. – PhD-student;
Romerovych-Misilak M. **–** Dr.Bio.Sci., Prof.

[1] V.S. Saji, H.C. Choe, K.W.K. Yeung, Int.J. Nano- and Biomaterials 3(2), 119 (2010).
[2] S.M. Moghimi, A.C. Hunter, J.C. Murray, FASEB J 19, 311 (2005).
[3] Muye Li, Fang Li, Zhicong He, Junpei Zhang, Junbo Han, Peixiang Lu, J. Appl. Phys.116, 233106 (2014).
[4] I. Fenoglio, B. Fubini, E.M. Ghibaudi, F.Turci, Adv. Drug Deliv. Rev.63, 1186 (2011).
[5] J.B. Blanco-Canosa, M. Wu, K. Susumu, E.Petryayeva, T.L. Jennings, P.E. Dawson, W.R. Algar, I.L. Medintz, Coord. Chem. Rev.263- 264, 101 (2014).
[6] Mingzhen Yao, Xing Zhang, Lun Ma, Wei Chen, Alan G. Joly, Jinsong Huang, Qingwu Wang, J. Appl. Phys.108, 103104 (2010).
[7] M. Gao, C. Lesser, S. Kirstein, H.Möhwald, A.L. Rogach, H. Weller, J. Appl. Phys.87, 2297 (2000).
[8] A.M. Derfus, W. Chan, S.N. Bhatia, Nano Lett. 4, 11 (2004).
[9] Q. Xiao, S. Huang, Z.D. Qi, B. Zhou, Z.K. He, Y. Liu, BBA-Proteins Proteome 1784, 1020 (2008).
[10] L.Shao, C.Dong, F.Sang, H.Qian, J.Ren, J. Fluoresc. 19, 151 (2009).
[11] Q. Xiao, S. Huang, W. Su, P. Li, J. Ma, F. Luo and Y. Liu, Colloids and Surfaces B: Biointerfaces 102, 76(2013).
[12] D. Wu, Z. Chen and X. Liu, Spectrochimica Acta part A: Molecular and Biomolecular Spectroscopy 84, 178 (2011).
[13] J. Hemmateenejad and S. Yousefinejad, J. Molecular Structure 1037, 317 (2013).
[14] E.A. Bhogale, N. Patel, J. Mariam, P.M. Dongre, A. Miotello, D.C. Kothari, Colloids and Surfaces B: Biointerfaces102, 257 (2013).
[15] H.H. Luu, Q. Kang, J. Kyung Park, W. Si, Q. Luo, W. Jiang, H. Yin, A.G. Montag, M.A. Simon, T.D. Peabody, R.C. Haydon, C.W. Rinker-Schaeffer, T.-C. He, Clinical & Experimental Metastasis22, 319 (2005).
[16] C. Cappadone, C. Stefanelli, E. Malucelli, M. Zini, C. Onofrillo, A. Locatelli, M. Rambaldi, A. Sargenti, L. Merolle, G. Farruggia, A. Graziadio, L. Montanaro, and S. Iotti, Biochem. Biophys. Res. Commun 467(2), 348(2015).
[17] C. Wang , Q. Ma , W. Dou , S. Kanwal, G. Wang, P. Yuan, and X. Su, Talanta 77(4), 1358 (2009).
[18] D.V. Korbytyak, S.M. Kalytchuk, I.I. Geru, J. Nanoelectronics and optoelectronics 4(1), 1 (2009).
[19] A.I. Savchuk, I.D. Stolyarchuk, P.M. Grygoryshyn, O.P. Antonyuk, and T.A. Savchuk, Proc. of SPIE 9066, 906618(2013).
[20] I.D. Stolyarchuk, O. A. Shporta, Physics and Chemistry of Solid State 17(4), 498 (2016).
[21] J.N. Tian, J.Q. Liu, W.Y. He, Z.D. Hu, X.J. Yao, and X.G. Chen, Biomacromolecules 5, 1956 (2004).
[22] J. Liang, Y. Cheng, and H. Han, J. Mol. Struct. 892, 116 (2008).
[23] A. Barth and P.I. Haris (Eds.), Biological and Biomedical Infrared Spectroscopy (IOS Press, 2009).
[24] A.I. Ivanov, R.G. Zhbankov, E.A. Korolenko, E.V. Korolik, L.A. Meleshchenko, M. Marchewka, and H. Ratajczak, J. Appl. Spectrosc. 60, 399 (1994).
[25] J. Coates, Interpretation of Infrared Spectra, A Practical Approach in: R.A. Meyers (Ed.) Encyclopedia of Analytical Chemistry (John Wiley & Sons Ltd, Chichester, 2000).
[26] J. Kong and S. Yu, Acta Biochim. Biophys. Sinica 39(8), 549 (2007).
[27] C. Ota, S. Noguchi, and K. Tsumoto, Biopolymers 103(4),237 (2015).
[28] S. Tabassum, W.M. Al-Asbahy, M. Afzal, and F. Arjmand, J. Photochem. Photobiol. B: Biology 114, 132(2012).

[29] Q. Wang, P. Liu, X. Zhou, X. Zhang, T. Fang, P. Liu, X. Min, and X. Li, J. Photochem. Photobiol. A: Chemistry230, 23 (2012).
[30] G. Walsh, Proteins: Biochemistry and Biotechnology (John Wiley & Sons, Chichester, 2002).
[31] Li-wei Liu, Si-yi Hu, Ying Pan, Jia-qi Zhang, Yue-shuFeng, and Xi-he Zhang, Beilstein J. Nanotechnol5, 919 (2014).
[32] Shen Zheng, Ji-Yao Chen, Jun-Yong Wang, Lu-Wei Zhou, and Qian Peng, J. Appl. Phys.110, 124701 (2011).
[33] Y. Zheng, S. Gao, and J.Y. Ying, Adv. Mater. 19, 376 (2007).
[34] A. Maureen Walling, J.A. Novak and J.R.E. Shepard, Int. J. Mol. Sci. 10, 441 (2009).

І.Д. Столярчук, Р. Войнаровська-Новак, Я. Політ, Є. Шерегій, С. Новак, М. Ромерович-Місілак

Квантові точки CdTeта їх біокон‘югати із альбуміном крові людини для флуоресцентної візуалізації

Методи оптичної спектроскопії використовувались для дослідження взаємодії між квантовими точками (КТ) CdTe з альбуміном крові людини (HSA), а також ефективність флуоресцентної візуалізації біокон'югатів КТ CdTe-HSA в порівнянні з колоїдними квантовими точками CdTe у ракових клітинах остеосаркоми людини. Вторинна структура HSA подібна нативній формі, що свідчить про біосумісність підготовлених біонанокомплексів. Біокон‘югати КТ CdTe-HSA демонструють хімічну стабільність в фосфатно-сольовомубуфері (PBS) в умовах навколишнього середовища та стабільність в цитоплазмі і підходять для маркування клітин, відстеження та іншої біовізуалізації. Квантові точки CdTe, розташовані в ракових клітинах остеосаркоми, демонструють високу інтенсивність люмінесценції. Інтенсивність випромінювання квантових точок CdTe, пов'язаних з альбуміном у біокомплекси, менша колоїдних квантових точок, але є задовільна і стабільна та має тривалий час фотолюмінесценції. Це свідчить про те, що біонанокомплекси КТ CdTe -HSA можуть використовуватись в якості флуоресцентного зонда для маркування ракових клітин, відстеження та інших застосувань у біовізуалізації.

Ключові слова: CdTe**,** квантова точка, наночастинка, альбумін крові людини, гасіння флуоресценції, ракові клітини остеосаркоми, біонанокомплекс, біокон‘югат, біовізуалізація.